Polymer Chemistry

Bilayer-Domain Formation of Thermoresponsive Amphiphilic Block Copolymers in Hybrid Liposomes for Synthetic Molecular Channels

Journal:	*Polymer Chemistry*
Manuscript ID	PY-ART-03-2023-000223.R1
Article Type:	Paper
Date Submitted by the Author:	10-Apr-2023
Complete List of Authors:	Ozawa, Naoki; Shinshu Daigaku Kosaka, Shunji; Shinshu Daigaku Fujii, Shota; University of Kitakyushu, Nishimura, Tomoki; Shinshu Daigaku, Department of Chemistry and Materials, Faculty of Textile Science and Technology

ARTICLE

Bilayer-Domain Formation of Thermoresponsive Amphiphilic Block Copolymers in Hybrid Liposomes for Synthetic Molecular Channels

Received 00th January 20xx,
Accepted 00th January 20xx

DOI: 10.1039/x0xx00000x

Naoki Ozawa, ‡[a] Shunji Kosaka, ‡[a] Shota Fujii, ¶[b] and Tomoki Nishimura *[a]

Molecularly permeable vesicles have attracted interest as compartments for nanoreactors or artificial cells, as they can allow the transport of molecules from the exterior to the interior of the vesicles. One strategy to increase vesicle permeability is the incorporation of amphiphilic copolymers that contain thermoresponsive poly(propylene oxide) into phospholipid vesicles. However, the nanostructures of these polymers, which are directly related to the molecular permeability, remain to be elucidated. Here, we report on the nanostructures of polymers incorporated in such membranes and the permeability of the polymer/phospholipid hybrid vesicles against water-soluble molecules. Neutron-scattering experiments revealed that the polymers form disk-like bilayer domains on the membranes, whose thickness is almost equivalent to that of the bilayer membranes when the polymers alone are self-assembled into vesicles. These domains act as synthetic molecular channels for low-molecular-weight poly(ethylene glycol), and their permeability can be regulated by changing the molecular weight of the poly(propylene oxide). These findings provide valuable insight into the design of novel polymers for synthetic channels, the prediction of their permeability, and the preparation of permeable vesicles.

Introduction

Hybrid vesicles composed of amphiphilic copolymers and phospholipids have attracted increasing attention in recent years due to the unique advantages they offer over traditional phospholipid vesicles.[1, 2, 3] The combination of properties from the polymers and phospholipids allows for a wide range of functionalities, such as biocompatibility, increased stability in aqueous solutions,[4, 5, 6] controlled release by external stimuli,[7, 8] and targeted delivery to specific organs or tissues.[9, 10] As a result, hybrid vesicles have been the subject of extensive research to understand their fundamental physical properties[11, 12, 13, 14, 15, 16, 17, 18] and to demonstrate their potential as carriers in drug -delivery systems and compartments for nanoreactors and artificial cells.[19, 20, 21, 22, 23]

In addition to the functionalities mentioned above, the incorporation of specific polymers into liposomes can endow the vesicles with bespoke permeability.[24, 25] We have already reported intrinsically permeable polymer vesicles composed of thermoresponsive amphiphilic copolymers containing poly(propylene oxide) (PPO),[18, 26, 27] polyoxazoline,[28] and a polypeptoid.[29] In particular, amphiphilic copolymers with PPO can be incorporated into phospholipid membranes, where they act as synthetic molecular channels for water-soluble molecules. The widespread use of liposomes or polymer vesicles as nanoreactors has so far been hindered by their low molecular permeability and the inability to allow the passage of substrates from the external environment to the interior of the vesicle.[30, 31] In contrast, the hybrid vesicles we have developed exhibit improved molecular permeability, and we have demonstrated their ability to function as enzymatic reactors in which substrates can be supplied from the outside. However, the nanostructures of the incorporated polymers on the phospholipid membranes have not yet been investigated systematically.

The permeability of the hybrid vesicles can be expected to be influenced by the distribution of the polymer on the hybrid membranes, for example, by a homogeneous polymer distribution or the formation of polymer-rich domains, as well as the nanostructures of the polymer domains, such as bilayer formation or a state of simple insertion in the phospholipid membranes. Thus, gaining a deeper understanding of the structural characteristics of these hybrid membranes could potentially be useful for controlling their permeability and designing PPO-based polymers that act as synthetic channels. Additionally, the minimum molecular weight of PPO required for amphiphilic polymers that contain PPO to be incorporated into these membranes remains unclear. Therefore, further study in these areas would be beneficial for the prediction of the permeability and the design of novel synthetic molecular channels.

[a] *Department of Chemistry and Materials, Faculty of Textile Science and Technology, Shinshu University, 3-15-1, Tokida, Ueda, Nagano 386-8567, Japan*
E-mail: nishimura_tomoki@shinshu-u.ac.jp
[b] *Department of Chemistry and Biochemistry, University of Kitakyushu, 1-1, Hibikino, Kitakyushu, Fukuoka 808-0135, Japan*
Electronic Supplementary Information (ESI) available. See DOI: 10.1039/x0xx00000x

‡These authors contributed equally to the work.

¶ *Present address:* Polymer Science and Engineering Department, University of Massachusetts, Amherst, Massachusetts 01003, United States

Here, we report on the nanostructure of maltopentaose-*b*-PPO incorporated in phospholipid vesicle membranes, which was examined using confocal laser scanning microscopy (CLSM), cryo-transmittance electron microscopy (cryo-TEM), and small-angle neutron scattering (SANS). Although the formation of polymer-rich domains could be observed using CLSM and cryo-TEM in the polymer/lipid hybrid membranes, the precise nanostructure of the incorporated polymers, specifically, whether they formed bilayers, could not be determined using these analytical methods. Consequently, an alternative technique, namely, contrast-matching SANS, was employed to investigate the structural information of the incorporated polymers. In contrast to the scattering of X-rays, which linearly increases with the atomic number, the scattering of neutron beams depends on the scattering length density (SLD) of the scattering nucleus. For example, there is a substantial difference in SLD between hydrogen and deuterium. Therefore, by mixing H_2O and D_2O in different proportions, the SLD of the solvent can be systematically varied and matched to the SLD of one of the components of the hybrid vesicle. By employing the technique known as contrast matching, it is possible to render a phospholipid invisible.[32, 33] Thus, contrast-matching SANS measurements are able to provide structural information exclusively from the incorporated polymers and should deliver hard experimental evidence for the formation of polymer-rich domains on the hybrid membrane and allow quantification of their size. Through this combination of techniques, we confirmed the presence of heterogeneous polymer-rich domains composed of bilayer disk-like shapes on the hybrid vesicle membranes and demonstrated the function of the incorporated polymers as synthetic molecular channels for a water-soluble molecule (**Fig. 1**).

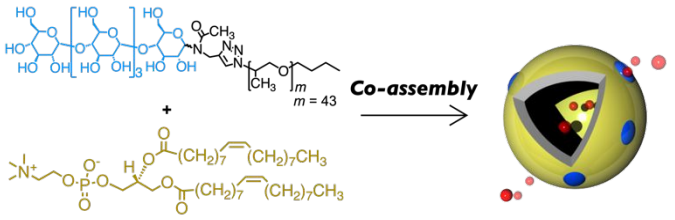

Fig. 1 Schematic illustration of the formation of polymer-rich domains that act as molecular channels in maltopetantaose-*b*-PPO/phospholipid hybrid vesicles.

Results and discussion

We first examined whether maltopentaose-*b*-PPO copolymers based on PPO with a molecular weight of 2.5K (henceforth referred to in this manuscript as maltopentaose-*b*-$PPO_{2.5K}$) could be incorporated into phospholipid membranes and form polymer-rich domains on the membranes. For this purpose, we attempted to prepare micrometer-sized vesicles as follows. Methanol solutions of maltopentaose-*b*-$PPO_{2.5K}$ and 1,2-dioleoyl-*sn*-glycero-3-phosphocholine (DOPC; the phase-transition temperature of DOPC is *ca.* –17 °C) were mixed in a molar ratio of 1 : 9, before the methanol was removed under an argon flow to afford polymer/phospholipid films. To enable the polymer and the phospholipid to be distinguished using CLSM, we added a small amount of rhodamine-labeled polymer and 7-nitrobenzofurazan (NBD)-labeled 1,2-dioleoyl-*sn*-glycero-3-phosphoethanol amine (DOPE) to the polymer/phospholipid mixture. After the addition of distilled water, the films were hydrated at 25 °C for 24 h to yield micrometer-sized vesicles. **Fig. 2a** shows a CLSM image of polymer/phospholipid vesicles that contain 10 mol% of the block copolymer at 25 °C. The rhodamine fluorescence was distributed over the vesicle, suggesting that the polymer was successfully incorporated into the phospholipid membrane. Moreover, the heterogeneous distribution of the rhodamine fluorescence within the membrane indicates the formation of polymer-rich microdomains. The phase separation of the polymer and DOPC on the hybrid bilayer membrane can be attributed to the large difference between the thickness of the hydrophobic layers of DOPC (2.25 nm) and that of the polymer bilayers (9.5 nm) (**Fig. S3** and **Table S1**). The mismatch in hydrophobic layers between DOPC and the polymer leads to the formation of domains and induces an increase in line tension at the phospholipid/polymer boundary. PPO has a low glass-transition temperature (T_g) and is flexible;[34] the conformation of the PPO polymer chain changed to match the thickness of the DOPC hydrophobic bilayer in order to reduce the line tension, which facilitated the formation of the stable polymer-rich domains. Moreover, the hybrid vesicles were stable, and the polymer-rich domain did not exhibit budding into the polymer vesicles after 72 h (**Fig. S4**). Such long-term stability would be advantageous for the use of the hybrid vesicles in materials applications.

To further investigate the formation of the polymer/phospholipid hybrid vesicles, we prepared micrometer-sized giant vesicles using polymer : DOPC molar ratios ranging from 2 : 8 to 9 : 1. The fluorescence of rhodamine was colocalized with that of NBD for all vesicles (**Figs. 2b–2i**), suggesting that the polymers can insert into the phospholipid membranes at any composition. Interestingly, distinct polymer-rich domains were present in the hybrid vesicles with polymer/phospholipid molar ratios of 2 : 8 to 4 : 6. When the polymer/phospholipid molar ratio reached 5 : 5, the clear microdomains observed in the hybrid vesicles with lower polymer ratios were no longer present. However, the fluorescence of rhodamine and NBD did not show large-scale heterogeneity for the hybrid vesicles with polymer/phospholipid compositions of 5 : 5 to 8 : 2, which was attributed to the formation of nanometer-sized polymer-rich domains on the phospholipid membranes. Thus, the formation of clear polymer-rich domains like those seen in **Figs. 2a–2e** depends on the molar fraction of the polymer in the hybrid vesicles. At low molar fractions of the polymer, few distinct polymer-rich domains are expected to be observed. In fact, sometimes no micrometer-sized domains were formed on some hybrid vesicles with polymer/phospholipid molar ratios of 1 : 9 to 5 : 5, and only nanometer-sized domains were observed (**Fig. S5**). This is due to the fact that the polymer/phospholipid composition cannot be controlled within

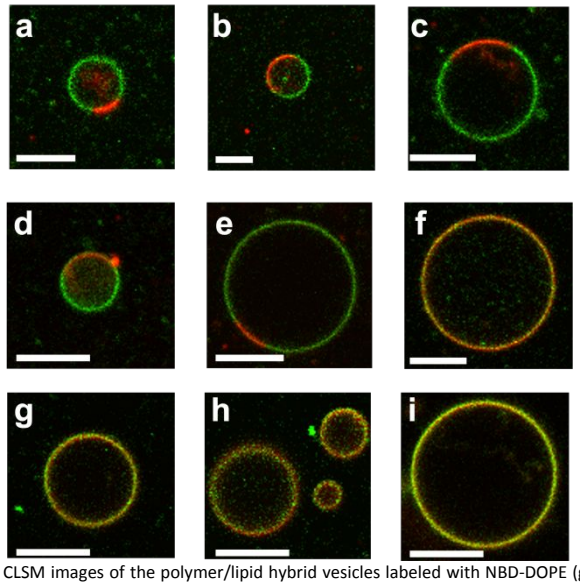

Fig. 2 CLSM images of the polymer/lipid hybrid vesicles labeled with NBD-DOPE (green channel) and rhodamine-polymer (red channel) with different molar ratios of maltopentaose-*b*-$PPO_{2.5K}$ and DOPC. a) [polymer] : [DOPC] = 1 : 9; b) = 2 : 8; c) = 3 : 7; d) = 4 : 6; e) = 5 : 5; f) = 6 : 4; g) = 7 : 3; h) = 8 : 2; i) = 9 : 1; scale bars = 10 μm.

the vesicle population because the vesicles are kinetic products.[35]

Having confirmed the formation of polymer-rich domains in the micrometer-sized giant hybrid vesicles, we next investigated the nanostructures of nanometer-sized polymer/DOPC hybrid vesicles using cryo-TEM. As a control experiment, we first performed cryo-TEM measurements on DOPC vesicle and maltopentaose-*b*-$PPO_{2.5K}$ polymer vesicle solutions. The solutions were prepared via film hydration followed by sequential extrusion using a polycarbonate membrane (pores: 0.1 μm) at 25 °C. Cryo-TEM images of both vesicle solutions showed spherical vesicular structures, with an average membrane thickness of *ca.* 2.5 nm and *ca.* 6.5–7 nm for the DOPC vesicle and polymer vesicles, respectively (**Figs. 3a and 3b**). We then carried out cryo-TEM measurements on hybrid vesicles with a maltopentaose-*b*-$PPO_{2.5K}$ polymer : phospholipid molar composition of 1 : 9 (**Figs. 3c and 3d**). Only spherical vesicular structures were observed; other nanostructures such as wormlike micelles and spherical micelles were not observed. Careful observation of the images revealed that the thicknesses of the vesicle membranes varies, whereby the thicker areas correspond to the polymer bilayer membranes and the thinner areas to the DOPC bilayer membranes. Moreover, a solution of hybrid vesicles with a maltopentaose-*b*-$PPO_{2.5K}$ polymer : phospholipid molar composition of 2 : 8 was also examined using cryo-TEM, and both thin membranes and thick membranes co-existed within the membrane of the same hybrid vesicle. Interestingly, the CLSM images show that the hybrid domain vesicles have only one polymer-rich domain. This may be due to the fusion of several polymer-rich domains that formed immediately after the vesicles were prepared. Indeed, the nanometer-sized vesicles observed immediately after preparation showed some polymer-rich domains on the membrane (**Fig. 3f**). To prepare the micron-sized hybrid vesicles, the polymer/phospholipid thin films were hydrated and agitated to form vesicles. During this incubation, the polymer-rich domains would coalesce to reduce the in-line tension at the polymer/phospholipid interface, resulting in the formation of a polymer-rich domain on the membrane. Here, we have observed hybrid vesicles of different sizes using CLSM and Cryo-TEM, However, the differences between the micrometer-sized vesicles and the nanometer-sized vesicles are not only in size but also in the curvature of the vesicles. The curvature of the vesicles could affect the thermodynamics of phase separation, such as the critical concentration of polymer required for phase separation and the size and stability of the resulting polymer-rich domains. In our system, vesicles of any size form polymer-rich domains and there is no size effect. However, their long-term stability remains unexplored and the effect of vesicle size on the stability of polymer-rich domains needs to be investigated. Overall, these data clearly suggest the presence of polymer-rich domains in the nanometer-sized hybrid vesicles.

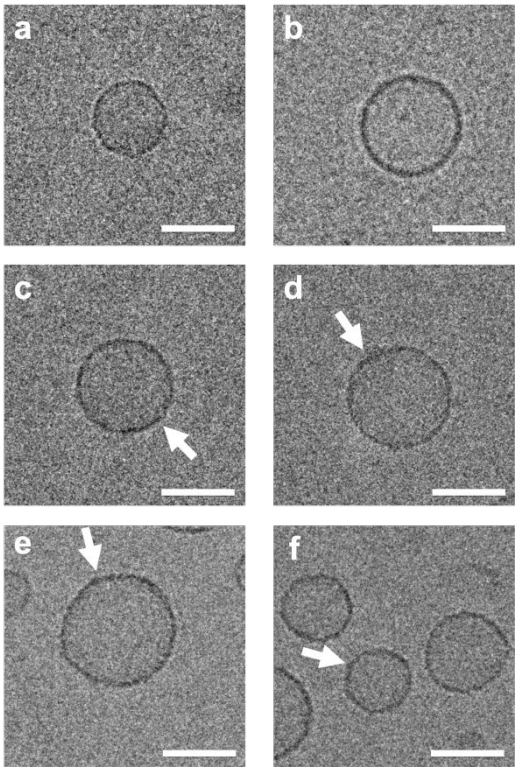

Fig. 3 Cryo-TEM images of a) a DOPC liposome, b) a maltopentaose-*b*-$PPO_{2.5K}$ polymer vesicle, c, d) polymer/lipid hybrid vesicles with a maltopentaose-*b*-$PPO_{2.5K}$: DOPC molar ratio of 1 : 9, and e, f) the polymer/lipid hybrid vesicles with a maltopentaose-*b*-$PPO_{2.5K}$: DOPC molar ratio of 2 : 8; white arrows indicate thicker membrane regions, which correspond to polymer bilayer membranes; scale bars = 50 nm.

The aforementioned studies confirmed that polymer-rich domains can be formed on the polymer/phospholipid hybrid vesicles. However, the CLSM and cryo-TEM observations are not able to paint a detailed picture of the nanostructures of these polymer-rich domains on the hybrid vesicles due to the limitations of their resolution. Therefore, it remained unknown at that point whether or not the polymers form bilayer structures in the domains and what their thickness is. To obtain further information regarding the nanostructure of these polymer-rich domain, we attempted to conduct a structural analysis of the hybrid vesicles using contrast-matching SANS measurements. For this purpose, we prepared a mixed solution of the polymer maltopentaose-*b*-$PPO_{2.5K}$ and 1,2-dimyristoyl-d_{54}-*sn*-glycero-3-phosphocholine (DMPC-d_{54}) with a polymer/phospholipid molar composition of 9 : 1. Since the SLD of DMPC-d_{54} matches that of a solvent consisting of D_2O and H_2O in an 86 : 14 ratio (**Fig. S6**),[36] it is possible to render the phospholipid invisible and obtain only structural information from the polymer-rich domain in the hybrid vesicles. We therefore used DMPC-d_{54} instead of DOPC. Before conducting the SANS measurements, we prepared the polymer/DMPC-d_{54} hybrid vesicles and confirmed that the polymers were incorporated into DMPC liposomes to form polymer-rich domains using CLSM (**Fig. S7)** and cryo-TEM (**Fig. S8)**. We then subjected the polymer/DMPC-d_{54} hybrid vesicles in 86 vol% D_2O (i.e., the contrast matching point of DMPC-d_{54}) at 30 °C, which is above the phase transition temperature of DMPC, to SANS measurements (**Fig. 4a**). The SANS profile of the hybrid vesicle solution does not show a distinct minimum like that seen in the SANS profile of the DMPC-d_{54} liposome solution, indicating that the scattering profile does not reflect the spherical vesicular structures. We then attempted to fit the SANS profile using a core–shell disk model to obtain information about the polymer-rich domains.[37, 38] The model fitted the SANS profile well over the entire *q*-range and was consistent with a disk radius of 38 nm, a hydrophobic layer thickness of 9.5 nm, and an overall thickness of 13.5 nm (**Fig. 4b**); these results clearly suggest that the polymer-rich phase forms disk-like bilayer structures. The overall thickness and the hydrophobic layer thickness of the polymer-rich domain are very similar to those of the bilayer of maltopentaose-*b*-$PPO_{2.5K}$ polymer vesicles (**Table S1**). The similar thickness of the domain and the bilayer of the polymer vesicles indicates that the conformation of the polymer chains in the domain is similar to that in the bilayer membrane. Although the SANS measurements prove that a disk-like polymer-rich domain is formed, the radius of the polymer-rich domain is somewhat large compared to the radius of the hybrid vesicles (60 nm by DLS). This might be attributed to the heterogeneous composition of the polymer and the phospholipid within each hybrid vesicle. It is difficult to achieve a uniform molar distribution when fabricating films composed of the polymers and DMPC, leading to the production of hybrid vesicles with either high-polymer or high-phospholipid compositions. This resulted in a large distribution in the size of the polymer-rich domains, resulting in larger domain sizes than we expected. A similar observation has also been reported by Le Meins *et al*.[35] More importantly, the SLD value of the hydrophobic layer in the domain (1.0×10^{10} cm^{-2}) was higher than the theoretical SLD value of PPO (0.34×10^{10} cm^{-2}).[39] Since the thickness of the hydrophobic layer did not change in the D_2O/H_2O solvent mixture, the enhancement of the SLD value can be attributed to the presence of D_2O in the hydrophobic layer. We have previously demonstrated that the permeability of maltopentaose-*b*-PPO vesicles is predominantly due to the partitioning in the hydrated hydrophobic layer.[40] The polymer domains with the hydrated hydrophobic layer are expected to act as synthetic molecular channels.

The formation of polymer-rich domains is facilitated by the large mismatch between the length of the polymer and the thickness of the hydrophobic layer of the lipids.[1] In fact, maltopentaose-*b*-$PPO_{2.5K}$ (hydrophobic layer thickness: 9.5 nm) formed polymer-rich domains on DOPC and DMPC liposomes, which exhibit a thickness of the hydrophobic layer between 2.25 nm and 2.55 nm. We then examined the effect of the hydrophobic layer thickness on the domain formation by using maltopentaose-*b*-PPO with a PPO molecular weight of 1.5K (henceforth referred to as maltopentaose-*b*-$PPO_{1.5K}$ in this manuscript). Maltopentaose-*b*-$PPO_{1.5K}$ self-assembled into spherical vesicles with a membrane thickness of 10.0 nm in water (**Fig. S9**) and was able to be incorporated into DOPC

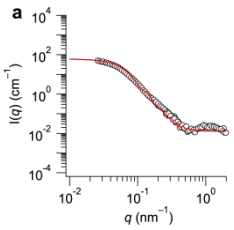

Parameters	
SLD of the hydrophilic region (cm^{-2})	1.00×10^{10}
SLD of the hydrophobic region (cm^{-2})	5.20×10^{10}
SLD of the solvent (cm^{-2})	5.35×10^{10}
Radius of the disk (nm)	38
Thickness of the hydrophobic region (nm)	9.5
Overall thickness of the disk (nm)	13.5
Standard deviation of the thickness of the disk	4.5

Fig. 4 a) SANS profile of the maltopentaose-*b*-$PPO_{2.5K}$/DMPC-d_{54} hybrid vesicles at 30 °C in 86 : 14 D_2O : H_2O (open circles) and theoretical curves obtained from the core–shell disk model (red line). b) Structural parameters of the polymer assemblies in the hybrid vesicles.

and DMPC liposomes, as evident from the results shown in **Fig. S10**. We then investigated the nanostructure of the maltopentaose-*b*-$PPO_{1.5K}$/DMPC-d_{54} hybrid vesicles under DMPC-d_{54}-matching conditions using SANS measurements and observed that the SANS profiles were consistent with the core–shell disk model (**Fig. S11**), indicating that maltopentaose-*b*-$PPO_{1.5K}$ also formed polymer-rich domains on the liposome membranes. PPO with a molecular weight of less than 1.5 K lacks sufficient hydrophobicity at room temperature to function as a hydrophobic segment of amphiphilic polymers and does not form stable molecular assemblies. Therefore, a molecular weight of 1.5 K is the minimum necessary for the incorporation of PPO into phospholipid membranes. The overall thickness of the domain (8.0 nm) is slightly smaller than that of the maltopentaose-*b*-$PPO_{1.5K}$ bilayer membrane (10 nm), potentially due to shrinkage of the hydrophobic PPO segments. However, further investigation is needed to fully understand the mechanism of this conformational change. Overall, these

findings clearly demonstrate that block copolymers that contain PPO with a hydrophobic layer thickness of 6–9.5 nm are conducive to the formation of polymer-rich domains on phospholipid membranes, and that these domains adopt a bilayer disk-like shape.

Having established that polymer-rich domains adopt bilayer disk-like morphologies on the phospholipid membranes, we subsequently examined the potential of these domains to act as synthetic channels on liposomes. Previous research has shown that maltopentaose-*b*-PPO self-assembles into molecularly permeable polymer vesicles. Consequently, we hypothesized that the incorporation of these polymers into phospholipid membranes would enhance their permeability. To test the permeability, we prepared solutions of micrometer-sized giant vesicles with a maltopentaose-*b*-$PPO_{2.5K}$: DOPC molar ratio of 1 : 9 and then added water-soluble fluorescein isothiocyanate conjugated poly(ethylene glycol)(FITC-PEG) with a molecular weight of 550. We then directly observed their fluorescence intensity profiles 5, 30, and 60 minutes after the addition of FITC-PEG. After five minutes, the FITC intensity inside the vesicle was about ~50% that outside the vesicle (**Fig. 5a**), and the intensity increased with increasing incubation time (**Fig. 5b**).

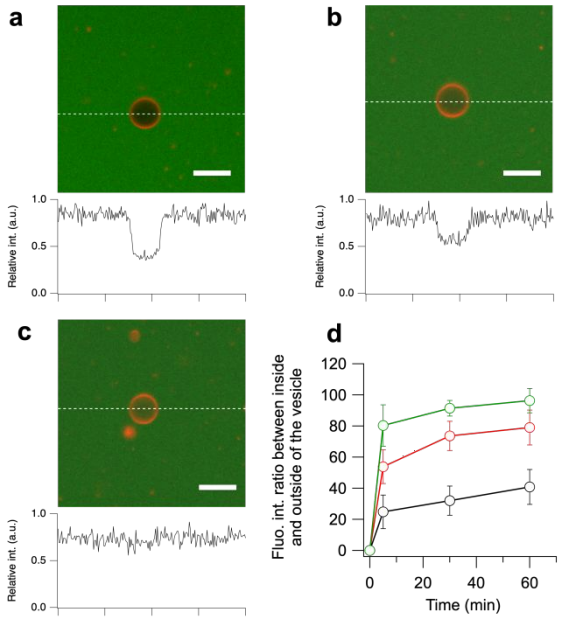

Fig. 5 Representative CLSM images of the maltopentaose-*b*-$PPO_{2.5K}$/DOPC hybrid vesicles labeled with rhodamine-DOPE (red channel) a) 5 min, b) 30 min, and c) 60 min. after the addition of FITC-PEG550 (green channel); scale bars = 10 μm. d) Changes in the ratio between the FITC fluorescence intensity inside and outside the maltopentaose-*b*-$PPO_{1.5K}$/DOPC hybrid vesicles (green open circles), maltopentaose-*b*-$PPO_{2.5K}$/DOPC hybrid vesicles (red open circles), and DOPC liposomes (black open circles) after 5 min, 30 min, and 60 min.

After one hour, the fluorescence intensity inside the vesicle reached *ca.* 80% relative to the outside fluorescence intensity (**Fig. 5c**). In contrast, the fluorescence intensity increased only slightly in the less-permeable DOPC liposomes (**Figs. 5d and S12**). These data clearly show that the incorporated polymers enhance the permeability of the hybrid liposomes toward hydrophilic FITC-PEG. We have previously reported that the permeation behavior of maltopentaose-*b*-PPO vesicles changes with temperature.[40] Therefore, the polymer domains incorporated into phospholipid bilayers are expected to show similar permeation behaviour as the polymer vesicles with respect to temperature. We further investigated the permeability of vesicles incorporating maltopentaose-*b*-$PPO_{1.5K}$ into DOPC liposomes to understand the effect of the molecular weight of the PPO chains of the block polymer on the permeability of the hybrid vesicles toward FITC-PEG. As expected, the permeability increased with decreasing molecular weight of PPO, i.e., with decreasing bilayer thickness (**Figs. 5d and S13**). According to Fick's first law, the permeability coefficient is proportional to the membrane thickness, and therefore, the permeability increased. Importantly, this result indicates that the permeability can be controlled by adjusting the molecular weight of the PPO chain. If amphiphlic copolymers with a high degree of polymerization PPO are used, the permeability of the artificial channels will decrease as the thickness of the polymer membrane increases due to Fick's first law. In addition, the interface between the phospholipid and polymer segments can generate a high interfacial tension, which can lead to instability and deformation of the vesicle structure. This would be further enhanced by the large size of the hydrophobic segment of the polymer, which can increase the interfacial tension at the interface. However, further studies are needed to obtain a more conclusive result. Overall, we have demonstrated that the polymers incorporated in the phospholipid membranes act as synthetic molecular channels for water-soluble molecules.

Conclusions

In conclusion, we have used CLSM and cryo-TEM to reveal the formation of heterogeneous polymer-rich domains upon the incorporation of maltopentaose-*b*-poly(propylene oxide) (PPO) with average bilayer membrane hydrophobic thicknesses of 6.0 nm or 9.5 nm into phospholipid vesicles. The resulting polymer-rich domains form disk-like bilayer structures, as verified by contrast-matching SANS experiments. The thicknesses of the polymer-rich domains were found to be very similar to those of the bilayer membranes when the polymers alone are self-assembled into spherical vesicles. We have also demonstrated that the polymer-rich domains act as synthetic molecular channels for water-soluble PEG with an average molecular weight of 550, transporting the molecules into the inner phase of the hybrid vesicles. This study thus provides design guidelines for novel synthetic molecular channels based on amphiphilic copolymers that contain PPO. Although many synthetic channels that allow the permeation of ions and water have already been reported,[41, 42, 43, 44] reports on synthetic channels that allow the permeation of molecules with molecular weights of several hundreds of Daltons are limited.[7, 8, 45] Therefore,

synthetic molecular channels based on polymers with PPO could facilitate the deployment of nanoreactors as therapeutic tools, e.g., for prodrug activation, and the development of compartments for novel artificial cell/organelle models.[31, 46, 47, 48]

Author Contributions

S.K. and N.O. contributed equally to this work. The manuscript was written through contributions of all authors. All authors have given approval to the final version of the manuscript.

Conflicts of interest

There are no conflicts to declare.

Acknowledgements

This work was supported by the JSPS via grants-in-aid for scientific research (B:22H02140, Exploratory:22K19057), the MEXT Leading Initiative for Excellent Young Researchers, the JST FOREST Program (JPMJFR201P), and the MEXT Promotion of Distinctive Joint Research Center Program (JPMXP0621467946). SAXS experiments were conducted at the BL40B2 beamline of SPring-8 under proposal numbers 2021A1065, 2021B1089, 2022A1095, and 2022B1109. SANS experiments were carried out via the JRR-3 general user program managed by the Institute for Solid State Physics at The University of Tokyo under proposal numbers 21542 and 22568.

References

1 Y. K. Go and C. Leal, *Chem. Rev.*, 2021, **121**, 13996-14030.
2 J. F. Le Meins, C. Schatz, S. Lecommandoux and O. Sandre, *Mater. Today*, 2013, **16**, 397-402.
3 M. Schulz and W. H. Binder, *Macromol. Rapid Commun.*, 2015, **36**, 2031-2041.
4 K. P. Mineart, S. Venkataraman, Y. Y. Yang, J. L. Hedrick and V. M. Prabhu, *Macromolecules*, 2018, **51**, 3184-3192.
5 S. Chatterjee and T. Ooya, *ACS Appl. Polym. Mater.*, 2020, **2**, 1909-1916.
6 M. Fauquignon, E. Ibarboure and J.-F. Le Meins, *Soft Matter*, 2021, **17**, 83-89.
7 S. C. Sebai, S. Cribier, A. Karimi, D. Massotte and C. Tribet, *Langmuir*, 2010, **26**, 14135-14141.
8 V. Passos Gibson, M. Fauquignon, E. Ibarboure, J. Leblond Chain and J.-F. Le Meins, *Polymers*, 2020, **12**, 637.
9 Z. Cheng, D. R. Elias, N. P. Kamat, E. D. Johnston, A. Poloukhtine, V. Popik, D. A. Hammer and A. Tsourkas, *Bioconjugate Chem.*, 2011, **22**, 2021-2029.
10 X. Su, S. K. Mohamed Moinuddeen, L. Mori and M. Nallani, *J. Mater. Chem. B*, 2013, **1**, 5751-5755.
11 T. Ruysschaert, A. F. P. Sonnen, T. Haefele, W. Meier, M. Winterhalter and D. Fournier, *J. Am. Chem. Soc.*, 2005, **127**, 6242-6247.
12 J. Nam, P. A. Beales and T. K. Vanderlick, *Langmuir*, 2011, **27**, 1-6.
13 M. Chemin, P.-M. Brun, S. Lecommandoux, O. Sandre and J.-F. Le Meins, *Soft Matter*, 2012, **8**, 2867-2874.
14 C. Magnani, C. Montis, G. Mangiapia, A.-F. Mingotaud, C. Mingotaud, C. Roux, P. Joseph, D. Berti and B. Lonetti, *Colloids Surf. B: Biointerfaces*, 2018, **168**, 18-28.
15 A. K. Khan, J. C. S. Ho, S. Roy, B. Liedberg and M. Nallani, *Polymers*, 2020, **12**, 979.
16 N. Hamada, S. Gakhar and M. L. Longo, *Biochim. Biophys. Acta. Biomembr.*, 2021, **1863**, 183552.
17 Y. K. Go, J. Shin, G. Chen and C. Leal, *Chem. Mater.*, 2022, **34**, 8577-8592.
18 R. Seneviratne, R. Catania, M. Rappolt, L. J. C. Jeuken and P. A. Beales, *Soft Matter*, 2022, **18**, 1294-1301.
19 A. Peyret, E. Ibarboure, J.-F. Le Meins and S. Lecommandoux, *Adv. Sci.*, 2018, **5**, 1700453.
20 M. Mohammadi, S. Taghavi, K. Abnous, S. M. Taghdisi, M. Ramezani and M. Alibolandi, *Adv. Funct. Mater.*, 2018, **28**, 1802136.
21 S. Khan, J. McCabe, K. Hill and P. A. Beales, *J. Colloid Interface Sci.*, 2020, **562**, 418-428.
22 F. Persano, G. Gigli and S. Leporatti, *Nano Express*, 2021, **2**, 012006.
23 V. De Leo, F. Milano, A. Agostiano and L. Catucci, *Polymers*, 2021, **13**, 1027.
24 W. Shen, J. Hu and X. Hu, *Chem. Phys. Lett.*, 2014, **600**, 56-61.
25 M. Fauquignon, E. Courtecuisse, R. Josselin, A. Mutschler, A. Brûlet, M. Schmutz and J.-F. Le Meins, *J. Colloid Interface Sci.*, 2021, **604**, 575-583.
26 T. Nishimura, Y. Sasaki and K. Akiyoshi, *Adv. Mater.*, 2017, **29**, 1702406.
27 T. Nishimura, S. Hirose, Y. Sasaki and K. Akiyoshi, *J. Am. Chem. Soc.*, 2020, **142**, 154-161.
28 T. Nishimura, N. Sumi, Y. Koda, Y. Sasaki and K. Akiyoshi, *Polym. Chem.*, 2019, **10**, 691-697.
29 Y. Okuno, T. Nishimura, Y. Sasaki and K. Akiyoshi, *Biomacromolecules*, 2021, **22**, 3099-3106.
30 D. E. Discher and A. Eisenberg, *Science*, 2002, **297**, 967-973.
31 T. Nishimura and K. Akiyoshi, *Adv. Sci.*, 2018, **5**, 1800801.
32 L. van't Hag, L. de Campo, C. J. Garvey, G. C. Feast, A. E. Leung, N. R. Yepuri, R. Knott, T. L. Greaves, N. Tran, S. L. Gras, C. J. Drummond and C. E. Conn, *J. Phys. Chem. Lett.*, 2016, **7**, 2862-2866.
33 R. Dos Santos Morais, O. Delalande, J. Pérez, L. Mouret, A. Bondon, A. Martel, M.-S. Appavou, E. Le Rumeur, J.-F. Hubert and S. Combet, *Langmuir*, 2017, **33**, 6572-6580.
34 J. Herzberger, K. Niederer, H. Pohlit, J. Seiwert, M. Worm, F. R. Wurm and H. Frey, *Chem. Rev.*, 2016, **116**, 2170-2243.
35 T. P. T. Dao, F. Fernandes, M. Er-Rafik, R. Salva, M. Schmutz, A. Brûlet, M. Prieto, O. Sandre and J.-F. Le Meins, *ACS Macro Lett.*, 2015, **4**, 182-186.
36 W. C. Leite, Y. Wu, S. V. Pingali, R. L. Lieberman and V. S. Urban, *J. Phys. Chem. Lett.*, 2022, **13**, 9834-9840.
37 S. Venkataraman, Z. A. Chowdhury, A. L. Lee, Y. W. Tong, I. Akiba and Y. Y. Yang, *Macromol. Rapid Commun.*, 2013, **34**, 652-658.
38 T. Nishimura, Y. Hatatani, M. Ando, Y. Sasaki and K. Akiyoshi, *Chem. Sci.*, 2022, **13**, 5243-5251.
39 R. L. Vekariya, V. K. Aswal, P. A. Hassan and S. S. Soni, *Langmuir*, 2014, **30**, 14406-14415.
40 T. Nishimura, L. de Campo, H. Iwase and K. Akiyoshi, *Macromolecules*, 2020, **53**, 7546-7551.
41 N. Voyer and M. Robitaille, *J. Am. Chem. Soc.*, 1995, **117**, 6599-6600.
42 M. Barboiu, *Angew. Chem., Int. Ed.*, 2012, **51**, 11674-11676.
43 S.-P. Zheng, L.-B. Huang, Z. Sun and M. Barboiu, *Angew. Chem., Int. Ed.*, 2021, **60**, 566-597.
44 J. Yang, G. Yu, J. L. Sessler, I. Shin, P. A. Gale and F. Huang, *Chem*, 2021, **7**, 3256-3291.
45 L. Messager, J. R. Burns, J. Kim, D. Cecchin, J. Hindley, A. L. B.

Pyne, J. Gaitzsch, G. Battaglia and S. Howorka, *Angew. Chem., Int. Ed.*, 2016, **55**, 11106-11109.
46 T. M. S. Chang, *Nat. Rev. Drug Discov.*, 2005, **4**, 221-235.
47 B. C. Buddingh' and J. C. M. van Hest, *Acc. Chem. Res.*, 2017, **50**, 769-777.
48. J. F. Mukerabigwi, Z. Ge and K. Kataoka, *Chem. – Eur. J.*, 2018, **24**, 15706-15724.